MgB_2-based negative refraction index metamaterial at visible frequencies: Theoretical analysis

Adil-Gerai Kussow,[1] Alkim Akyurtlu,[2] Andrey Semichaevsky,[2] and Niwat Angkawisittpan[2]
[1]*Department of Physics, University of Massachusetts, Lowell, Massachusetts 01854, USA*
[2]*Electrical and Computer Engineering Department, University of Massachusetts, Lowell, Massachusetts 01854, USA*
(Received 29 January 2007; revised manuscript received 12 July 2007; published 26 November 2007)

The presented metamaterial consists of the matrix (magnesium diboride MgB_2 in a normal state, at room temperature) with randomly (or regularly) embedded spherical nanoparticles of a polaritonic crystal, SiC. The calculations demonstrate explicitly that the metamaterial exhibits negative refraction index behavior with low losses for a scattered wave. The result stands for *both* random and regular distributions of SiC nanoparticles inside the MgB_2 matrix. This favorable situation stems from the Drude-like behavior of both the low-energy, $p_2(\omega_{p_2} \approx 1.9$ eV), and the high-energy, $p_1(\omega_{p_1} \approx 6.3$ eV), plasmon modes of MgB_2 with plasmon losses, $\gamma \leqslant 0.25$ eV. The effective medium parameters were calculated in the framework of the extended theories of Maxwell-Garnett [Philos. Trans. R. Soc. London, Ser. A **203**, 385 (1904)] and Lewin [Proc. Inst. Electr. Eng. **94**, 65 (1947)], and the obtained results are validated via *ab initio* finite difference time domain simulations.

DOI: 10.1103/PhysRevB.76.195123 PACS number(s): 73.20.Mf, 74.70.−b, 42.25.Bs, 41.20.Jb

I. INTRODUCTION

There has been renewed interest in the properties of materials with negative index of refraction (NIMs), originally proposed in early papers of Veselago,[1] Mandel'shtam,[2] Lamb,[3] and Shuster.[4] Since a material with a negative refraction index, $n<0$, exactly reverses the propagation paths of rays within it,[5] it has the advantage to form low reflectance surfaces by canceling the scattering properties of other materials. This property will permit, in principle, the perfect lens or a planar slab of NIM.[6,7] The study of NIMs began in the microwave regime,[6] then moved into the terahertz,[8,9] and then into the infrared regions.[10] In recent years, due to the development of nanotechnology, a long-awaited breakthrough in the optical, mostly near-infrared range of frequencies, was reported on NIMs.[11–18]

In this paper, we report the MgB_2-based design for a NIM within the visible frequency range. Our sample is a mixture of two dielectric media: the matrix and the inclusions. The matrix consists of polycrystalline magnesium diboride (MgB_2). Since the polycrystal material, due to the averaging the optical response over the randomly oriented crystallites, has no directional dependence, it is optically isotropic. It is well known that in an optically isotropic situation, the resultant dielectric tensor is reduced to the *scalar* dielectric function $\varepsilon(\omega)$.[19] The MgB_2 matrix serves as a host material for SiC spherical inclusions. Two arrangements of the spherical inclusions embedded into the polycrystalline MgB_2 host matrix were considered: (1) the polaritonic nanoparticles (SiC) with the same radius, r_{SiC}, are embedded randomly[20,21] and (2) the particles are embedded regularly into the matrix with the fill factor f. In the situation of a regular arrangement, the inclusions constitute a simple cubic lattice (Lewin's model[22]). It should be noted that our structure is different from the structure suggested in Ref. 23. In this reference, *two* types of spheres were arranged on two interpenetrating simple cubic lattices. In our design, only *one* type of spheres (SiC) is utilized and, moreover, these inclusions are embedded both regularly (arrangement 1) and randomly (arrangement 2) into the matrix of *homogeneous* MgB_2.

The negative refraction index was achieved by a combination of the effective medium theories and the rigorous finite difference time domain (FDTD) method. The effective medium theories, i.e., Maxwell-Garnett extended theory for random arrangement (can be obtained by Mie theory[21]) and Lewin's theory[22] (for regular arrangement), were used to properly adjust the parameters of the metamaterial. Afterward, the result was tested by FDTD simulations. The Mie resonance due to SiC inclusions was observed at some frequency range, $\Delta\omega_{\mu_{eff}<0}$, with the effective permeability negative, i.e., $\mu_{eff}<0$. Due to the plasmon Drude-like behavior of the MgB_2 matrix, the effective permittivity is negative, i.e., $\varepsilon_{eff}<0$, within another frequency range, $\Delta\omega_{eff<0}$. The adjustment of the fill factor f and the radius of the SiC sphere r_{SiC} was utilized to make these regions overlap to reach the negative refraction index behavior within the visible region where both ε_{eff} and μ_{eff} are negative.

In the proposed metamaterial at optical frequencies, the matrix compound should satisfy two requirements. Firstly, the permittivity $\varepsilon(\omega)$ should obey a Drude-like behavior with a plasmon frequency ω_p within the optical frequency range (or higher):

$$\varepsilon(\omega) = \varepsilon_\infty - \frac{\omega_p^2}{\omega^2 + i\gamma\omega}, \tag{1}$$

where ω is the frequency of the incident plane wave, ε_∞ is the high-frequency dielectric constant, and γ is the loss rate. Secondly, the losses γ should be small. Otherwise, the scattered wave with some effective (negative) index of refraction, i.e., $\mathrm{Re}(n_{eff})<0$, will suffer large losses, i.e., $k = \left|\frac{\mathrm{Im}(n_{eff})}{\mathrm{Re}(n_{eff})}\right| \geqslant 1$. Many recently reported NIMs in the optical frequency range exhibit a large loss factor, $k \sim 1$,[12,15] mostly due to the fact that noble metals (Au, Ag) were utilized as the hosts for the metamaterials. Since noble metals have considerable plasmon losses[24] and since the typical fill factor for metal is not small ($f \geqslant 0.2$), the loss factor for a scattered wave is large, i.e., $k \geqslant 1$. Our design of the metamaterial utilizes the recently discovered superconductor material,

MgB_2, instead of a noble metal as a matrix. The host medium of our metamaterial is the MgB_2 polycrystal, with both theoretically and experimentally verified low plasmon losses (see below). Since the plasmon losses are very sensitive to the defect structure of the MgB_2, we have carefully analyzed the stability of the negative refraction index effect with respect to the magnitude of the losses γ within the entire experimentally reported range.

It should be mentioned that the superconductor-based metamaterials have been reported recently[25,26] in NIM designs, but in the ~10 GHz (or lower) frequency range. Moreover, the metamaterials[25,26] require a low temperature. Our metamaterial does not need this requirement and reveals the negative refraction index effect even at room temperature.

The plan of the paper is as follows. Our main objective is to validate the negative refraction index effect in the proposed MgB_2-based metamaterial. Since, as an input parameter, the optical calculations require the dielectric functions, we will describe first the dielectric function $\varepsilon(\omega)$ of the host, MgB_2. We should stress that $\varepsilon(\omega)$ was taken from the available literature. Secondly, the effective medium theories and the FDTD formalisms, which allow us to calculate the optical parameters, are described. Finally, the results of the optical calculations are discussed and a comparison of the negative refraction index bands for different models of the dielectric function of MgB_2 is conducted.

II. DIELECTRIC FUNCTION OF THE MgB_2

A. Two plasmon modes

The discovery of superconductivity in MgB_2 with T_c of 39 K has generated much scientific interest in recent years,[27–41] and considerable amount of data on the physical properties of MgB_2 are now available. MgB_2 belongs to the so-called AlB_2 structure in which B atoms form graphitelike honeycomb layers that alternate with hexagonal layers of Mg atoms. The plasmon parameters of MgB_2 are a controversial issue.[39] Despite the theoretical prediction[29] of the high magnitude of the plasmon frequency $\omega_p \approx 7$ eV (p_1 mode), many researches have reported a much smaller value: $\omega_p \approx 2$ eV in p_2 mode (both experimentally[34,37] and theoretically[28–33]). Moreover, as follows from the recently published experimental data of Fudamoto and Lee,[40] both plasmon modes coexist in a polycrystalline phase of MgB_2, since their energy ranges are well separated. In order to cover all of the possible ranges of the reported optical plasmon parameters of MgB_2, we have conducted two separate sets of calculations of the refraction index of our MgB_2-based metamaterial, for both the low-energy and the high-energy dielectric functions generated by the appropriate plasmons.

B. Low-energy plasmon mode

The *ab initio* MgB_2 band structure calculations[28–33] have demonstrated a low-energy plasmon mode, $\omega_{p_2}^{ab}$, where the B layers are parallel to the $\{a,b\}$ plane and the c direction corresponds to relatively weak interactions between the B layers.[28] The low-energy plasmon mode $p_2(\omega_{p_2}^{ab} \simeq 2.6$ eV) is twice degenerated plasmon in the $\{a,b\}$ plane.[39] The appropriate low plasmon losses $\gamma \leqslant 0.01$ eV in the low-energy plasmon mode were calculated in Ref. 33 by using *ab initio* time-dependent density-functional theory. The experimental data on both polycrystalline and single crystals of MgB_2 (Refs. 34–40) correlate with the theoretical results[33] for the frequency of the low-energy plasmon mode, $\omega_{p_2} \simeq 2.5$ eV, but the plasmon losses are much larger, given by $\gamma \approx 0.02-0.25$ eV. The experimental data on optical conductivity in the low-frequency plasmon mode can be adequately described by the Drude expression given by Eq. (1) with $\varepsilon_\infty \approx 1$, the plasma frequency, $\omega_p \approx 1.68$ eV, and the loss factor in the *ab* plane, $\gamma \approx 0.02$ eV.[34] Similar results for low-energy Drude dielectric function with $\omega_p \approx 2.0-2.5$ eV were also reported by other theoretical and experimental works.[33,37,40] The low-energy Drude dielectric function is a reasonable approximation which describes the (degenerated) *a-b* diagonal components of the permittivity tensor only within some *narrow* frequency window $\Delta\omega \sim 1.0$ eV centered at ~2 eV.[34] As follows from the experimental data,[34] the low-energy plasmon exists with a Drude-like dielectric function in a wide temperature range, 45–295 K, which includes both the superconducting and the normal states. It should be mentioned that the third component of the permittivity tensor ε_{ij} in the c direction is virtually frequency independent[39] (within the narrow frequency window mentioned above). The aforementioned Drude parameters are in reasonable agreement with the data on the polycrystalline sample:[37] $\omega_p = 1.39$ eV and $\gamma \approx 0.03$ eV. As was reported recently,[38,39] in the situation of a single MgB_2 crystal, the measured losses are actually much larger: $\gamma \approx 0.12-0.25$ eV. This enhancement of losses is due to the additional scattering of electrons by the defects [the loss rate γ of the Drude expression (1) is extremely sensitive to the sample purity[39]].

C. Losses (low-energy plasmon)

Since there is still some uncertainty regarding the level of losses in MgB_2 for the low-energy plasmon mode in the current literature[28–41] (different defect structures due to the fabrication, different methods of measurements, etc.), we have conducted three sets of optical calculations assuming the low-energy plasmonic dielectric function: (1) the polycrystalline MgB_2 matrix where the scattering due to the defects is neglected, and the losses are assumed to be the ideal theoretical losses[33] averaged over the orientation of grains. Since the situation with very small plasmon losses is far from the "real" experiments where defects contribute a lot into the losses,[38] we have conducted two additional calculations: (2) the polycrystalline MgB_2 matrix with a moderately developed defect structure and low-energy plasmon losses ~10 times larger than the theoretical losses[33] and (3) the highly defected matrix of polycrystalline MgB_2 with extremely large level of experimentally reported losses[38] ~100 times larger than the theoretical losses.

D. Dielectric function of polycrystalline MgB_2

The optical properties of the optically isotropic polycrystalline MgB_2 matrix are described by the frequency-depen-

dent dielectric function $\varepsilon(\omega)$ (Ref. 19) or the effective scalar permittivity. Consequently, we utilize the *averaged* MgB_2 single crystal permittivity tensor ε_{ij} assuming randomly oriented spherical grains with the same (averaged) size l. Since the typical size of the grains $l \sim 1-5$ μm (Ref. 37) in MgB_2 is larger than the wavelength in the visible region, the scalar permittivity of the MgB_2 polycrystal can be obtained by averaging the permittivities of the differently oriented grains (monocrystals) over their orientations: $\varepsilon=(1/3)\mathrm{Tr}\{\bar{\varepsilon}_{ik}\}$.[19,42]

In the first set of calculations, we have utilized the idealized theoretical Drude parameters for the low-energy plasmon mode: $\omega_p=\bar{\omega}_p=1.93$ eV, $\gamma=0.002$ eV.[33] The averaged effective plasmon frequency $\bar{\omega}_p \approx 1.93$ eV is the result of the calculation of the effective scalar permittivity ε or the permittivity tensor averaged over randomly oriented spherical grains. The *single crystal* tensor ε_{ij} (which is used in the averaging procedure) is isotropic only in the *ab* plane in the hexagonal system of coordinates $\varepsilon_{\xi\xi}=\varepsilon_{\zeta\zeta}$ (with ξ,ζ axes in the *ab* plane), and each component in the *ab* plane is described by a Drude-like expression [Eq. (1)] with $\varepsilon_\infty=1$. The third component (z is in the c direction) of the tensor $\varepsilon_{zz} \approx 1.6$ is actually frequency independent.[39] The appropriate effective scalar dielectric function ε due to the averaging over the orientation of the polycrystalline grains is expressed as a Drude dependence with the plasmon frequency $\bar{\omega}_p = \sqrt{2/3}\omega_{\xi\xi} \approx 1.93$ eV [$\omega_{\xi\xi} \approx 2.4$ eV (Ref. 39)] and $\varepsilon_\infty=1.2$. In the second set of calculations (moderately developed defect structure and moderate losses), the Drude parameters, $\omega_p \approx 1.68$ eV, $\gamma \approx 0.02$ eV, as found in the literature[34] were used. In the third set of calculations (well-developed defect structure), the extremely large Drude losses ($\gamma \approx 0.25$ eV) were utilized from the recent works of Refs. 39 and 40.

In contrast to the low-energy plasmon, the *high-energy* plasmon is almost isotropic, with all three degenerated frequencies given by $\omega_{p1}^c \approx \omega_{p1}^{ab} \simeq 6.3$ eV, $\varepsilon_\infty \approx 3.2$, and considerable (averaged over the polycrystalline gains) Drude losses $\gamma \approx 0.12$ eV.[39] The high-energy plasmon mode describes the dielectric function between $\sim$7.0 and $\sim$2.0 eV, and the low-energy plasmon mode between $\sim$1.0 and $\sim$2.0 eV.[40]

III. EFFECTIVE MEDIUM THEORIES

Again, our metamaterial is based on SiC spherical inclusions with radii r_{SiC} which are embedded into the MgB_2 matrix with the fill factor f. The radii and the fill factor constitute the design parameters and are used to calculate the effective permittivity ε_{eff}, the effective permeability μ_{eff}, and the effective refraction index n_{eff} of the sample. The permittivity of the SiC spherical inclusions, within the visible range of frequencies, was taken as $\varepsilon_{\mathrm{SiC}}=6.8+0.01i$.[43,44] Here, some small ($\sim$0.1%) losses are added [the experimental losses in SiC are smaller than 1% (Ref. 43)].

The calculations were initially carried out using the extended Maxwell-Garnett and Lewin theories.[21–23] According to the extended Maxwell-Garnett theory,[20,21,23] the effective medium permittivity ε_{eff} and permeability μ_{eff}, which describe the scattering of light (with the wavelength λ in vacuum) by randomly distributed particles, are given by

$$\varepsilon_{eff}=\varepsilon_h \frac{x^3-3ifT_I^E}{x^3+\frac{3}{2}ifT_I^E}, \tag{2}$$

$$\mu_{eff}=\mu_h \frac{x^3-3ifT_I^H}{x^3+\frac{3}{2}ifT_I^H}, \tag{3}$$

with the following electric-dipole T_I^E component and the magnetic-dipole T_I^H component of the scattering matrix of a single sphere:

$$T_I^E=\left[\frac{j_1(x_s)[xj_1(x)]'\varepsilon_s - j_1(x_s)[x_sj_1(x_s)]'\varepsilon_h}{h_1(x)[x_sj_1(x_s)]'\varepsilon_h - j_1(x_s)[xh_1(x)]'\varepsilon_s}\right], \tag{4}$$

$$T_I^H=\left[\frac{j_1(x_s)[xj_1(x)]'\mu_s - j_1(x_s)[x_sj_1(x_s)]'\mu_h}{h_1(x)[x_sj_1(x_s)]'\mu_h - j_1(x_s)[xh_1(x)]'\mu_s}\right]. \tag{5}$$

Here, $x=2\pi r|\sqrt{\varepsilon_h\mu_h}|/\lambda$, $x_s=2\pi r|\sqrt{\varepsilon_s\mu_s}|/\lambda$, r is the radius of the inclusions, and $j_1(x)$ and $h_1(x)$ are the spherical Bessel and Hankel functions of the first order, respectively. $\varepsilon_{h,s}$ and $\mu_{h,s}$ are the permittivity and the permeability of the host (h subscript) and of the inclusions (s subscript). Since at optical frequencies (and higher) the materials are principally nonmagnetic,[45] the permeability is given by $\mu_{h,s}=1$.

According to Lewin's theory,[22] the ε_{eff} and μ_{eff} for scattering of light by a simple cubic lattice of spherical inclusions are given by

$$\varepsilon_{eff}=\varepsilon_h\left(1+\frac{3f}{\frac{F(\theta)+2b_\varepsilon}{F(\theta)-b_\varepsilon}-f}\right), \tag{6}$$

$$\mu_{eff}=\mu_h\left(1+\frac{3f}{\frac{F(\theta)+2b_\mu}{F(\theta)-b_\mu}-f}\right), \tag{7}$$

with the function $F(\theta)$, $\theta=x_s$, fill factor f, and the parameters b_ε and b_μ:

$$F(\theta)=\frac{2(\sin\theta-\theta\cos\theta)}{(\theta^2-1)\sin\theta+\theta\cos\theta}, \tag{8}$$

$$b_\varepsilon=\frac{\varepsilon_h}{\varepsilon_s}, \quad b_\mu=\frac{\mu_h}{\mu_s}. \tag{9}$$

It should be noted that the parameter $x=2\pi r_{\mathrm{SiC}}|\sqrt{\varepsilon_h\mu_h}|/\lambda \ll 1$ should be small (otherwise, the effective medium theories fail to describe the scattering problem adequately). The calculated values for the x parameter were found to be $x \sim 0.1-0.2 \ll 1$, within the wavelengths of interest. These small values justify the criteria of validity of the effective medium theories. Moreover, since in the limit $x \to 0$ the Maxwell-Garnett and Lewin theories coincide exactly,[23] the solutions for $x \sim 0.1-0.2$ are close to each other, as can be seen in the following results.

It may be pointed out here that according to well-known results,[23,44,46] Eqs. (2)–(9), based on Mie theory, lead to a

negative effective permeability, $\mathrm{Re}(\mu_{eff})<0$, within an appropriate range of values for the following parameters: r, λ, $\varepsilon_{s,h}$, and f. This effect can be explained as follows. Due to the large permittivity of the spheres $\varepsilon_s>1$, there is an enhancement of the displacement current inside the inclusions. In its turn, this current causes the magnetic activity near the lowest TE resonance. As a result, the local magnetization attains the sign opposite to the magnetic field **H** of the electromagnetic wave. Finally, these local magnetic modes will produce a macroscopic (bulk) magnetization with negative magnetic permeability $[\mathrm{Re}(\mu_{eff})<0]$. The fundamental or first Mie magnetic resonance frequency $\omega_m^{res}=\pi c/r\sqrt{\varepsilon_s}$ can be expressed as the ratio between the wavelength in vacuum at resonance λ_m^{res} and the radius of the sphere r as follows: $r\sqrt{\varepsilon_s}/\lambda_m^{res}=0.5$. Due to the long-wavelength limit $x\ll 1$ (i.e., $r<\lambda_m^{res}$), which is needed for the validity of the effective medium theories,[21,22] this condition requires large permittivity of the spheres $\varepsilon_s>1$ (in our situation, SiC with $\varepsilon_s=6.8$). Our numerical calculations below explicitly demonstrate the described effect of the negative permeability, due to the adjusted size of the inclusions and fill factor, to satisfy the Mie resonance condition above.

IV. FINITE DIFFERENCE TIME DOMAIN CALCULATIONS

In order to further test the validity of Lewin-Maxwell-Garnett calculations, FDTD analysis of the scattering problem was conducted. It was assumed that SiC particles have a complex permittivity that obeys a simple model for a lossy medium with conductivity, σ_{SiC}, implemented as FDTD method for lossy dielectric media.[47] The Drude model for MgB_2 was implemented using FDTD-PLRC (piecewise linear recursive convolution) technique,[48] following the general PLRC methodology. The implementation of the semi-infinite simple cubic lattice of spheres (Lewin's arrangement) was based on the PEC (perfect electric conductor) and/or PMC (perfect magnetic conductor) periodic boundary conditions, with the grid terminated with UPML (uniaxial perfectly matched layer) on both sides, and the transmitted and reflected fields are sampled for the same polarization as the incident field. The sampled fields are then used to find the reflection S_{11} and the transmission S_{12} coefficients. The coefficients S_{11} and S_{12}, in turn, are employed in the calculation of the ε_{eff} and μ_{eff} from the extraction procedure.[49] The spherical inclusions with radii r_{SiC} are embedded into the MgB_2 matrix with the fill factor f. The radii and the fill factor constitute the free parameters and are used to calculate the ε_{eff}, μ_{eff}, and n_{eff}.

V. RESULTS

A. Low-energy plasmon mode

(a) Defects are excluded (low losses). Figure 1(a) displays the optical calculation results generated by the low-energy plasmon mode ($r_{\mathrm{SiC}}=120$ nm and $f=0.3$). These results correspond to the "ideal" polycrystalline MgB_2 matrix where the additional losses due to the scattering of electrons by defects are excluded (smallest plasmon losses). From this figure, the NIM bands occur in the visible range within the 620 and 655 nm for random arrangement and within 620 and 660 nm for regular arrangement. One can see that the negative refraction index band, as calculated by the FDTD model, appears within the same region as Lewin's arrangement between approximately 620 and 665 nm.

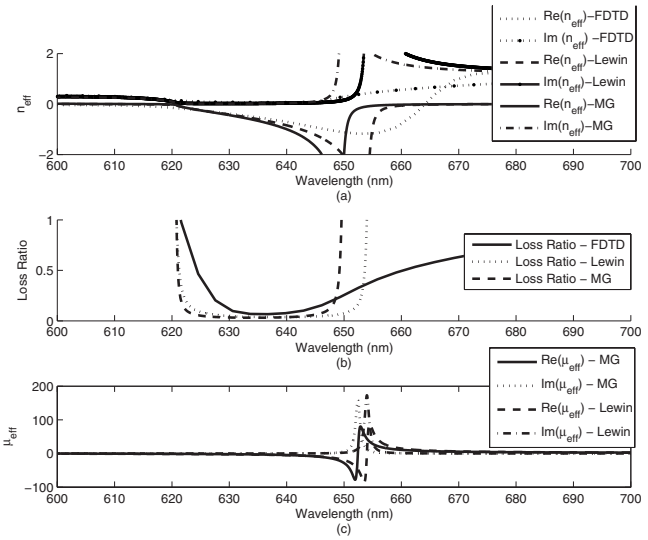

FIG. 1. Extended Maxwell-Garnett (MG), Lewin, and FDTD calculation results for (a) the real, $\mathrm{Re}(n_{eff})$, and imaginary, $\mathrm{Im}(n_{eff})$, parts of the effective index of refraction n_{eff}, (b) the loss ratio $k=|\mathrm{Im}(n_{eff})|/|\mathrm{Re}(n_{eff})|$, and (c) the real, $\mathrm{Re}(\mu_{eff})$, and imaginary, $\mathrm{Im}(\mu_{eff})$, parts of the effective permeability μ_{eff}. The metamaterial parameters (low-energy plasmon dielectric function, polycrystalline MgB_2 with no defects) are as follows: low plasmon losses $\gamma=0.002$ eV, $\omega_p=1.93$ eV, $r_{\mathrm{SiC}}=120$ nm, $\varepsilon_{\mathrm{SiC}}=6.8+0.01i$, and $f=0.3$.

The characteristic parameter of the effective wave attenuation (or loss ratio), $k=|\mathrm{Im}(n_{eff})/\mathrm{Re}(n_{eff})|$, is less than 1 within most of the NIM band (620–655 nm), with very low numbers ($k<0.2$) in the 630–645 nm region, as shown in Fig. 1(b) for the Maxwell-Garnett, Lewin, and FDTD models. Figure 1(c) is included to show the negative permeability as described in the previous section.

(b) Defects are included with moderate density. In the second set of calculations, which correspond to moderate losses (polycrystalline MgB_2 matrix with moderately developed defect structure), the Drude parameters, $\omega_p=1.68$ eV and $\gamma=0.02$ eV, were obtained from the averaging of the experimental single crystal data[34] over polycrystalline grain orientation ($r_{\mathrm{SiC}}=150$ nm, $f=0.3$) The optical calculation results are demonstrated in Fig. 2. The NIM behavior is observed within the 750–825 nm range for Lewin's model and 750–850 nm for FDTD. The loss ratios for both Lewin and FDTD models are still very low (~0.2) within the same frequency range (~750–820 nm) and less than 1 in the entire NIM band.

(c) Defects are included with high density. In order to further test the stability of our model for even higher losses, in our third set of calculations, we have used the following parameters: $\omega_p=2.0$ eV, $\gamma=0.25$ eV,[39,40] $f=0.3$, and $r_{\mathrm{SiC}}=150$ nm. As was mentioned above, this situation corre-

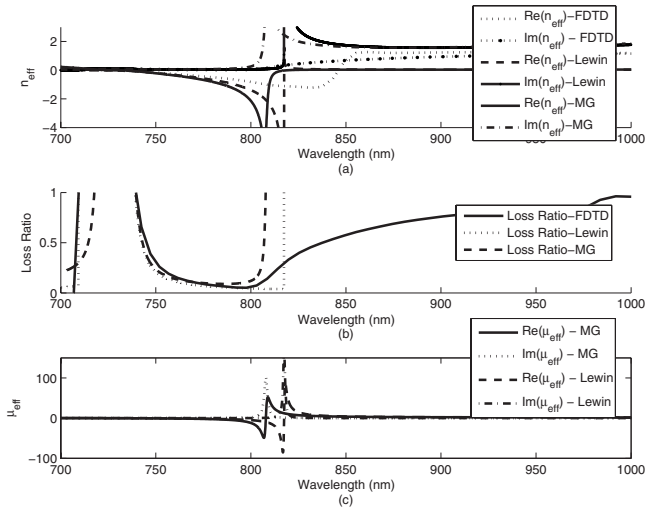

FIG. 2. Extended MG, Lewin, and FDTD calculation results for (a) the real, $\mathrm{Re}(n_{eff})$, and imaginary, $\mathrm{Im}(n_{eff})$, parts of the effective index of refraction n_{eff}, (b) the loss ratio $k=|\mathrm{Im}(n_{eff})|/|\mathrm{Re}(n_{eff})|$, and (c) the real, $\mathrm{Re}(\mu_{eff})$, and imaginary, $\mathrm{Im}(\mu_{eff})$, parts of the effective permeability μ_{eff}. The metamaterial parameters are as follows: $\omega_p=1.68$ eV, $\gamma=0.02$ eV, $\varepsilon_{\mathrm{SiC}}=6.8+0.01i$, $r_{\mathrm{SiC}}=150$ nm, and $f=0.3$ (low-energy plasmon dielectric function, polycrystalline MgB_2 matrix with enhanced losses).

sponds to the MgB_2 host as a highly defected matrix.[38] Again, in this situation with extremely high losses, both the FDTD and Lewin models predict a negative refraction index band within ~700–870 and ~700–825 nm, respectively, as shown in Fig. 3(a). The loss ratios of both the models are less than 1 in the entire band and less than 0.5 within most of the band.

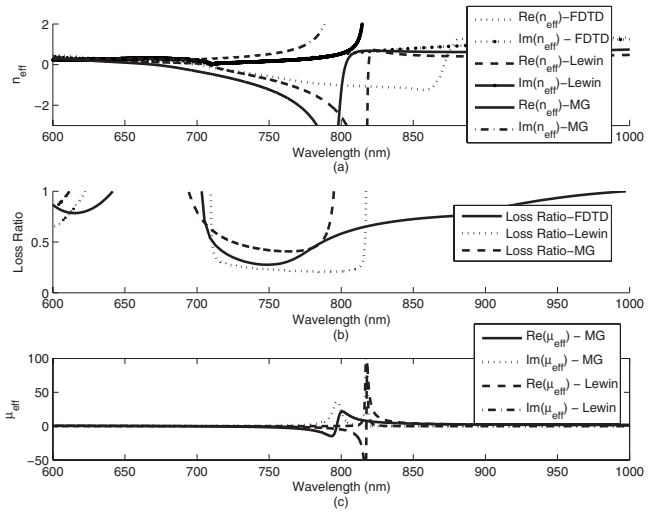

FIG. 3. Extended MG, Lewin, and FDTD calculation results for (a) the real, $\mathrm{Re}(n_{eff})$, and imaginary, $\mathrm{Im}(n_{eff})$, parts of the effective index of refraction n_{eff}, (b) the loss ratio $k=|\mathrm{Im}(n_{eff})|/|\mathrm{Re}(n_{eff})|$, and (c) the real, $\mathrm{Re}(\mu_{eff})$, and imaginary, $\mathrm{Im}(\mu_{eff})$, parts of the effective permeability μ_{eff}. The metamaterial parameters are as follows: $\omega_p=2.0$ eV, $\gamma=0.25$ eV, $\varepsilon_{\mathrm{SiC}}=6.8+0.01i$, $f=0.3$, and $r_{\mathrm{SiC}}=150$ nm (low-energy plasmon dielectric function, polycrystalline MgB_2 matrix with high plasmon losses).

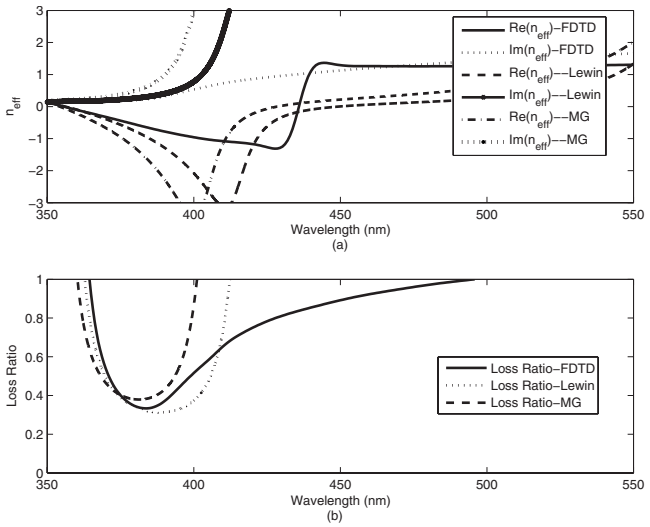

FIG. 4. (a) Extended MG, Lewin, and FDTD calculation results for (a) the real, $\mathrm{Re}(n_{eff})$, and imaginary, $\mathrm{Im}(n_{eff})$, parts of the effective index of refraction n_{eff} and (b) the loss ratio $k=|\mathrm{Im}(n_{eff})|/|\mathrm{Re}(n_{eff})|$. The metamaterial parameters (high-energy plasmon dielectric function) are as follows: $\omega_p=6.3$ eV, $\gamma=0.1$ eV, $r_{\mathrm{SiC}}=70$ nm, $\varepsilon_{\mathrm{SiC}}=8.0+0.1i$, and $f=0.3$.

B. High-energy plasmon mode: High losses

We also analyzed the situation when the high-energy, ~6.3 eV, plasmon mode of MgB_2 generates the dielectric function discussed above. Since the appropriate negative refraction index band is centered at the visible/UV edge, in this specific calculation, the permittivity of the SiC spheres was taken as $=8.0+0.1i$.[43] Figure 4 displays the results of the FDTD and effective medium calculations, with parameters $\omega_p=6.3$ eV,[40] $\gamma=0.1$ eV, $r_{\mathrm{SiC}}=70$ nm, and $f=0.3$. It can be seen that there is a negative refraction index band in the visible regime with acceptable loss ratios ($\leqslant 0.5$).

VI. DISCUSSION

We have analyzed our metamaterial optical response for both low-energy and high-energy dielectric functions of the MgB_2 host, with experimentally verified plasmon frequencies and corresponding levels of losses. As follows from the results (Figs. 1–4), the negative refraction index effect exists inside the visible regime for all scenarios, if the size and fill parameters of the metamaterial are adjusted.

In all of the situations considered, the negative refraction bands are well pronounced ($|n_{eff}| \geqslant 1$) with the bandwidths around 10 nm and small loss ratios. The main difference is the *position* of the negative index bands. The low-energy plasmon dielectric function generates the negative refraction index band in the visible close to the red edge, and the high-energy plasmon generates the band close to the visible/UV edge. It should be noted that the low-energy plasmon mode and the high-energy plasmon mode could, in principle, coexist. This coexistence stems from the fact that they are well separated in energy scale with $\Delta E \sim 4$ eV and describe independently the dielectric function in different frequency

ranges. Indeed, both simultaneously coexisting plasmon modes were reported recently in an experiment.[40] Hence, the metamaterial could produce negative refraction index effect on both ends of the visible spectrum, depending on the size of the SiC inclusions (r_{SiC}=70 nm for the visible/UV edge and r_{SiC}=150 nm for the red edge).

It should be mentioned that the losses in MgB_2 are very sensitive to fabrication processes, which affect the defect structure,[37–41] and hence can vary in a wide range. Since even the unfavorable scenario (Fig. 3) with *largest possible losses* known from the existing literature (~100 times larger than the theoretical losses) provides the NIM band with loss ratios less than 0.5, we believe that the proposed metamaterial is a good candidate for practical applications.

As we have already mentioned, the negative refraction index effect in our metamaterial is based on combining the Mie resonance and the plasmon Drude resonance to reach the effective negative permeability and permittivity simultaneously. The main difference between the NIM designs[23,46,50] based on a similar approach and our metamaterial is the usage of a MgB_2 matrix with extremely low loss plasmon mode located within the visible range of frequencies. According to the theoretical calculations (Ref. 33), this favorable MgB_2 plasmon low-loss situation is a consequence of both strong dynamic screening of the low-energy plasmon mode and the lack of particle-decay channels, due to the large energy gap ~5.0 eV.

VII. CONCLUSIONS

The proposed negative index metamaterial is the mixture of SiC nanoparticles and the polycrystalline MgB_2 in a normal state at room temperature. The design parameters are adjusted to produce the negative index of refraction band in the visible regime for both the low-energy and the high-energy plasmonic dielectric functions. Negative refraction index effect exists not only in the situation of a regular lattice arrangement of nanoparticles but also for randomly distributed nanoparticles. The main advantages of the proposed metamaterial are the optical isotropy and the low level of losses in a scattered wave: we were capable to achieve two to three times smaller losses than in other noble-metal-based metamaterials in the optical frequency range.[12,15] Similar level of losses was also reported recently[13,14] in the near-infrared region, and not in the visible regime. The proposed metamaterial is optically isotropic: the negative refraction index effect does not require special directions of the incident plane wave with respect to the surface of the sample. This property is a consequence of the constituents of the metamaterial: the optically isotropic polycrystalline MgB_2 matrix and spherical (hence isotropic) SiC inclusions. We believe that the favorable combination of both low losses and optical isotropy makes the metamaterial attractive for applications.

[1] V. G. Veselago, Sov. Phys. Usp. **10**, 509 (1968).
[2] L. I. Mandel'shtam, Zh. Eksp. Teor. Fiz. **15**, 475 (1945).
[3] H. Lamb, Proc. London Math. Soc. **1**, 473 (1904).
[4] A. Schuster, *An Introduction to the Theory of Optics* (Edward Arnold, London, 1904).
[5] D. R. Smith and N. Kroll, Phys. Rev. Lett. **85**, 2933 (2000).
[6] J. B. Pendry, A. J. Holden, D. J. Robbins, and W. J. Stewart, IEEE Trans. Microwave Theory Tech. **47**, 2075 (1999).
[7] J. B. Pendry, Phys. Rev. Lett. **85**, 3966 (2000).
[8] N. Wongkasem, A. Akyurtlu, K. A. Marx, W. D. Goodhue, J. Li, Q. Dong, and E. T. Ada, Microsc. Res. Tech. **70**, 497 (2007).
[9] T. J. Yen, W. J. Padilla, N. Fang, D. H. Vier, D. R. Smith, J. B. Pendry, D. N. Basov, and X. Zhang, Science **303**, 1494 (2004).
[10] M. S. Wheeler, J. S. Aitchison, and M. Mojahedi, Phys. Rev. B **73**, 045105 (2006).
[11] A. Semichaevsky, A. G. Kussow, A. Akyurtlu, and A. Karakashian, in *Proceedings of Metamaterials' 2007 First International Congress on Advanced Electromagnetic Materials in Microwaves and Optics*, Rome, 2007.
[12] Shuang Zhang, Wenjun Fan, Kevin J. Malloy, Steven R. J. Brueck, Nicolae C. Panoiu, and Richard M. Osgood, J. Opt. Soc. Am. B **23**, 434 (2006).
[13] Shuang Zhang, Wenjun Fan, N. C. Panoiu, K. J. Malloy, R. M. Osgood, and S. R. J. Brueck, Opt. Express **14**, 6778 (2006).
[14] Alexander V. Kildishev, Wenshan Cai, Uday K. Chettiar, Hsiao-Kuan Yuan, Andrey K. Sarychev, Vladimir P. Drachev, and Vladimir M. Shalaev, J. Opt. Soc. Am. B **23**, 423 (2006).
[15] A. Alu, A. Salandino, and N. Engheta, Opt. Express **14**, 1557 (2006).
[16] A. N. Grigorenko, A. K. Geim, H. F. Gleeson, Y. Zhang, A. A. Firsov, I. Y. Khrushchev, and J. Petrovic, Nature (London) **438**, 335 (2005).
[17] Gunnar Dolling, Christian Enkrich, Martin Wegener, Costas M. Soukoulis, and Stefan Linden, Science **312**, 892 (2006).
[18] G. Dolling, M. Wegener, A. Shadle, S. Burger, and S. Linden, Appl. Phys. Lett. **89**, 231118 (2006).
[19] M. Born and E. Wolf, *Principles of Optics* (Pergamon, Oxford, 1999).
[20] J. C. Maxwell and B. A. Garnett, Philos. Trans. R. Soc. London, Ser. A **203**, 385 (1904).
[21] W. T. Doyle, Phys. Rev. B **39**, 9852 (1989).
[22] L. Lewin, Proc. Inst. Electr. Eng. **94**, 65 (1947).
[23] V. Yannopapas and A. Moroz, J. Phys.: Condens. Matter **17**, 3717 (2005).
[24] P. B. Johnson and R. W. Christy, Phys. Rev. B **6**, 4370 (1972).
[25] M. Ricci, N. Orloff, and S. M. Anlage, Appl. Phys. Lett. **87**, 034102 (2005).
[26] A. Pimenov, P. Przyslupski, A. Loidl, and B. Dabrowski, Phys. Rev. Lett. **95**, 247009 (2005).
[27] J. Nagamatsu, N. Nakagawa, T. Muranaka, Y. Zenitani, and J. Akimitsu, Nature (London) **410**, 63 (2001).
[28] V. P. Zhukov, V. M. Silkin, E. V. Chulkov, and P. M. Echenique, Phys. Rev. B **64**, 180507(R) (2001).
[29] J. Kortus, I. I. Mazin, K. D. Belashchenko, V. P. Antropov, and L. L. Boyer, Phys. Rev. Lett. **86**, 4656 (2001).
[30] Amy Y. Liu, I. I. Mazin, and Jens Kortus, Phys. Rev. Lett. **87**,

087005 (2001).
[31] Y. Kong, O. V. Dolgov, O. Jepsen, and O. K. Andersen, Phys. Rev. B **64**, 020501(R) (2001).
[32] J. M. An and W. E. Pickett, Phys. Rev. Lett. **86**, 4366 (2001).
[33] Wei Ku, W. E. Pickett, R. T. Scalettar, and A. G. Eguiluz, Phys. Rev. Lett. **88**, 057001 (2002).
[34] J. J. Tu, G. L. Carr, V. Perebeinos, C. C. Homes, M. Strongin, P. B. Allen, W. N. Kang, Eun-Mi Choi, Hyeong-Jin Kim, and Sung-Ik Lee, Phys. Rev. Lett. **87**, 277001 (2001).
[35] A. V. Pronin, A. Pimenov, A. Loidl, and S. I. Krasnosvobodtsev, Phys. Rev. Lett. **87**, 097003 (2001).
[36] P. C. Canfield, D. K. Finnemore, S. L. Bud'ko, J. E. Ostenson, G. Lapertot, C. E. Cunningham, and C. Petrovic, Phys. Rev. Lett. **86**, 2423 (2001).
[37] A. B. Kuz'menko, F. P. Mena, H. J. A. Molegraaf, D. Van der Marel, B. Gorshunov, M. Dressel, I. I. Mazin, J. Kortus, O. V. Dolgov, T. Muranaka, and J. Akimitsu, Solid State Commun. **121**, 479 (2002).
[38] S. I. Krasnosvobodtsev, A. V. Varlashkin, A. I. Golovashkin, and N. P. Shabanova, Phys. Solid State **47**, 1600 (2005) [Fiz. Tverd. Tela **47**, 1541 (2005)].
[39] V. Guritanu, A. B. Kuzmenko, D. van der Marel, S. M. Kazakov, N. D. Zhigadlo, and J. Karpinski, Phys. Rev. B **73**, 104509 (2006).
[40] Y. Fudamoto and S. Lee, Phys. Rev. B **68**, 184514 (2003).
[41] T. Kakeshita, S. Lee, and S. Tajima, Phys. Rev. Lett. **97**, 037002 (2006).
[42] D. Stroud, Phys. Rev. B **12**, 3368 (1975).
[43] *Handbook of Optical Constants of Solids* (Academic, New York, 1998), Vols. I–III.
[44] K. C. Huang, M. L. Povinelli, and John D. Joannopoulos, Appl. Phys. Lett. **85**, 543 (2004).
[45] E. M. Lifshitz, L. D. Landau, and L. P. Pitaevskii, *Electrodynamics of Continuous Media*, 2nd ed., Course of Theoretical Physics Vol. 8 (Elsevier Butterman-Heinemann, Oxford, 1984).
[46] Christopher L. Holloway, Edward F. Kuester, James Baker-Jarvis, and Pavel Kabos, IEEE Trans. Antennas Propag. **51**, 2596 (2003).
[47] Allen Taflove and Susan C. Hagness, *Computational Electrodynamics: The Finite-Difference Time-Domain Method* (Artech House, Boston, 2000).
[48] D. F. Kelley and R. J. Luebbers, IEEE Trans. Antennas Propag. **44**, 792 (1996).
[49] W. Weir, Proc. IEEE **62**, 33 (1974).
[50] Byoung-Joon Seo, Tetsuya Ueda, Tatsuo Itoh, and Harold Fetterman, Appl. Phys. Lett. **88**, 161122 (2006).